Charmed meson resonances from Lattice QCD

Excited QCD 2024

Nicolas Lang
18/01/2024

Universidad de Valencia

Most hadrons are resonances!

Stable in iso-symmetric QCD:

- Mesons: $q\bar{q}$ states
  - Light: π, K, η
  - Heavy: D, D_s, B, B_s, B_c
- Baryons: qqq states
  - Light: N, Λ, Σ, Ξ, Ω
  - Heavy: Λ_c, ..., Ξ_{cc}, ..., Λ_b

Everything else are resonances!

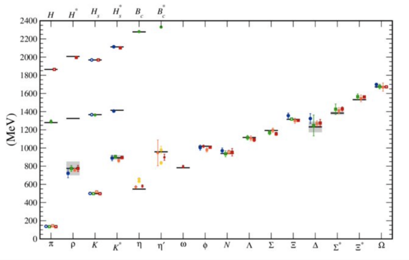

[Kronfeld, 1203.1204]

We would like to understand hadron resonances within QCD,
i.e. be as model-independent as possible.

Newly discovered hadrons since 2011

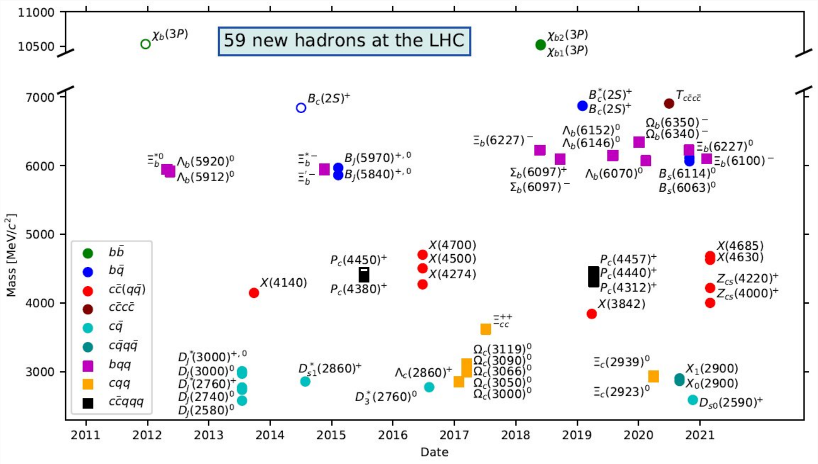

Credit: LHCb/CERN

How to get this from the lattice?

Even if the lattice does its job well it's still a different physical system!

Lattice:

- Finite volume
  $\rightarrow$ discrete spectrum
- Invariant under lattice translations and (subgroups of) the cubic group
- Euclidean field theory; no direct access to dynamics

Continuum:

- Infinite volume
  $\rightarrow$ continuous spectral density (branch cut singularities)
- Invariant under Poincare transformations
- Field theory in Minkowski space

Steps in the calculation

- Lattice discretization of QCD
- "Realistic operators"
  - Quantum numbers
  - Subduction
  - Spatial smearing
- Computing spectrum in finite box
- Relating the spectrum to amplitudes
- Parametrising amplitudes
- Fitting and finding poles

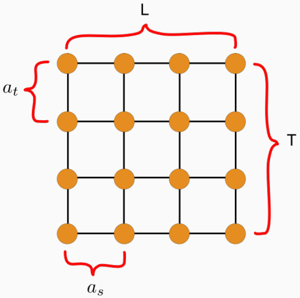

Computing observables on the lattice

Observables defined through euclidean path integral:

$$\langle \mathcal{O} \rangle = \frac{1}{Z} \int \mathcal{D}[q,\bar{q}]\mathcal{D}[U] e^{-S_F[q,\bar{q},U]-S_G[U]} \mathcal{O}[q,\bar{q},U] \; .$$

Fermionic part: analytic solution by Grassmann integration

$$\langle \mathcal{O} \rangle = \frac{1}{Z} \int \mathcal{D}[U] e^{-S_G[U]} \det D[U] \underbrace{\mathcal{O}_F[U, G[U]]}_{\langle \mathcal{O} \rangle_F} \; .$$

Gluonic part: numerical solution by importance sampling of gauge configurations

$$\langle \mathcal{O} \rangle = \langle \langle \mathcal{O}_F \rangle \rangle_G = \lim_{N_{\mathrm{cfgs}} \to \infty} \frac{1}{N_{\mathrm{cfgs}}} \sum_{i=1}^{N_{\mathrm{cfgs}}} \mathcal{O}_F[U_i, G[U_i]] \; .$$

Here we are interested in correlation functions of meson-interpolating operators:

$$\begin{aligned} C_{ij}(t) &\equiv \langle 0 | \mathcal{O}_i(t) \mathcal{O}_j^\dagger(0) | 0 \rangle \\ &= \sum_{n=1}^{\infty} \langle 0 | e^{Ht} \mathcal{O}_i(0) e^{-Ht} | n \rangle \langle n | \mathcal{O}_j^\dagger(0) | 0 \rangle \\ &= \sum_{n=1}^{\infty} e^{-E_n t} Z_i^n Z_j^{n*} \; , \end{aligned}$$

Computing the spectrum: Variational Method

- Assume we have a basis of operators interpolating a given set of quantum numbers
- Correlator matrix:

$$C_{ij}(t) = \langle 0|\mathcal{O}_i(t)\mathcal{O}_j^\dagger(0)|0\rangle \,,$$

- Find "optimal" interpolators by solving *Generalised Eigenvalue* (GEV) problem

$$C_{ij}(t)v_j^{(\mathfrak{n})} = \lambda_{\mathfrak{n}}(t,t_0)C_{ij}(t_0)v_j^{(\mathfrak{n})},$$

- This defines variationally-optimal operators:

$$\Omega_n^\dagger \equiv \sum_{i=1}^{N} v_i^n \mathcal{O}_i^\dagger$$

- Fit Principal correlators (eigenvalues):

$$\lambda_{\mathfrak{n}}(t,t_0) = (1-A_{\mathfrak{n}})e^{-E_{\mathfrak{n}}(t-t_0)} + A_{\mathfrak{n}}e^{-E'_{\mathfrak{n}}(t-t_0)}$$

- Some freedom in choice of t_0 and fitting range
- Stability w.r.t. operator basis should be tested

Meson operator bases

- Quark bilinears:

$$\bar{q}(\vec{x},t)\mathbf{\Gamma}_t^{Jm} q(\vec{x},t)$$

- Single mesons with definite flavour and momentum:

$$\mathcal{O}^{\dagger\, Jm}_{\boldsymbol{F}\nu}(\vec{p},t) = \sum_{\vec{x}} e^{i\vec{p}\cdot\vec{x}} \sum_{\nu_1,\nu_2} \mathcal{C}_{\mathrm{SU(3)}} \begin{pmatrix} \bar{\mathbf{3}} & \mathbf{3} & \boldsymbol{F} \\ \nu_1 & \nu_2 & \nu \end{pmatrix} \bar{q}_{\nu_1}(\vec{x},t)\mathbf{\Gamma}_t^{Jm} q_{\nu_2}(\vec{x},t)$$

- Meson-meson:

$$\Omega^{\dagger\, Jm}_{\boldsymbol{F}\nu}(\vec{P},t;[p_1,p_2]) = \sum_{\substack{\nu_1,\nu_2 \\ m_1,m_2}} \mathcal{C}_{\mathrm{SU(3)}} \begin{pmatrix} \boldsymbol{F}_1 & \boldsymbol{F}_2 & \boldsymbol{F} \\ \nu_1 & \nu_2 & \nu \end{pmatrix} \mathcal{C} \begin{pmatrix} J_1 & J_2 & J \\ m_1 & m_2 & m \end{pmatrix} \times \sum_{\substack{\vec{p}_i \in \{\, \vec{p}_i \,\}^* \\ \vec{p}_1 + \vec{p}_2 = \vec{P}}} \Omega^{\dagger\, J_1 m_1;}_{1\boldsymbol{F}_1\nu_1}(\vec{p}_1,t)\, \Omega^{\dagger\, J_2 m_2;}_{2\boldsymbol{F}_2\nu_2}(\vec{p}_2,t)$$

- Ω_i are variationally optimal operators

Lattice symmetries

Continuum: Poincaré symmetry
$\rightarrow$ Lattice: lattice translations
and (subgroups of) the cubic group

- Irrep of continuum rotation group is reducible representation of O_h (and subgroups)
- Can expand $\mathcal{O}^{Jm}$ in irreps of O_h (or subgroups)
- Inverting this expansion defines subduction to lattice irreps:

$$\mathcal{O}^{\dagger\,\Lambda\mu;[J]}_{\boldsymbol{F}\nu}(\vec{p},t) = \sum_m \mathcal{S}^{J,m}_{\Lambda,\mu}\,\mathcal{O}^{\dagger\,Jm}_{\boldsymbol{F}\nu}(\vec{p},t)$$

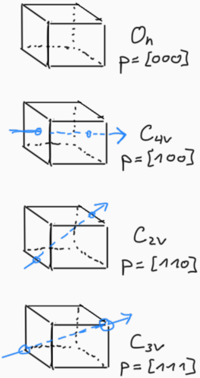

Subduced meson-meson operator:

$$\mathcal{O}^{\dagger\,\Lambda\mu}_{\boldsymbol{F}\nu}(\vec{P},t;[p_1,p_2]) = \sum_{\substack{\nu_1,\nu_2\\ \mu_1,\mu_2}} \mathcal{C}_{\mathrm{SU(3)}}\begin{pmatrix} \boldsymbol{F}_1 & \boldsymbol{F}_2 & \boldsymbol{F} \\ \nu_1 & \nu_2 & \nu \end{pmatrix} \mathbb{C}\begin{pmatrix} \Lambda_1^{\vec{p}_1} & \Lambda_2^{\vec{p}_2} & \Lambda^{\vec{P}} \\ \mu_1 & \mu_2 & \mu \end{pmatrix}$$

$$\times \sum_{\substack{\vec{p}_i\in\{\,\vec{p}_i\,\}^*\\ \vec{p}_1+\vec{p}_2=\vec{P}}} \mathcal{O}^{\dagger\,\Lambda_1\mu_1;}_{1\,\boldsymbol{F}_1\nu_1}(\vec{p}_1,t)\,\mathcal{O}^{\dagger\,\Lambda_2\mu_2;}_{2\,\boldsymbol{F}_2\nu_2}(\vec{p}_2,t)$$

Subduction Table

$\vec{d}$	G	Λ	J^P $(\vec{P}=\vec{0})$ $\lvert\lambda\rvert^{(\tilde{\eta})}$ $(\vec{P}\neq\vec{0})$	${}^1\ell_J$	${}^3\ell_J$
[000]	O_h	A_1^+	0^+, ...	${}^1S_0$	
		A_2^+	3^+, ...		${}^3D_3$
		E^+	2^+, ...	${}^1D_2$	${}^3D_2$
		T_1^+	1^+, 3^+, ...		$({}^3S_1, {}^3D_1)$, ${}^3D_3$
		T_2^+	2^+, ...	${}^1D_2$	${}^3D_2$, ${}^3D_3$
		A_1^-	0^-, ...		${}^3P_0$
		A_2^-	3^-, ...	...	...
		E^-	2^-, ...		${}^3P_2$
		T_1^-	1^-, 3^-, ...	${}^1P_1$	${}^3P_1$
		T_2^-	2^-, ...		${}^3P_2$

O_h: Lattice symmetry group at rest

Steps in the calculation

- Lattice discretization of QCD ✓
- "Realistic operators" ✓
  - Quantum numbers ✓
  - Subduction ✓
  - Spatial smearing ✓
- Computing spectrum in finite box ✓
- Relating the spectrum to amplitudes
- Parametrising amplitudes
- Fitting and finding poles

Quantization condition

In a generic QFT we have:

$$\det\left[\mathbf{1} + i\boldsymbol{\rho}(s)\cdot \boldsymbol{t}(s)\cdot(\mathbf{1} + i\boldsymbol{\mathcal{M}}(s,L))\right] = 0$$

[Original derivation: M. Lüscher; many extensions e.g. Sharpe, Briceño...]

- $\rho(s) = 2k(s)/\sqrt{s}$ with $k(s)$ the COM-momentum function and $s = E_{\mathrm{CM}}^2$
- $\boldsymbol{t}(s)$ = infinite volume t-matrix
- $\boldsymbol{\mathcal{M}}(s,L))$ encodes finite-volume effects
- $\boldsymbol{t}(s)$ is diagonal in total angular momentum J
- $\boldsymbol{\mathcal{M}}(s,L))$ is dense in J

When is this applicable?

- Arbitrary $2 \to 2$ scattering processes
- Box needs to be big enough: $L > 2R$ with $R \sim 1/m_\pi$
  Corrections exponentially suppressed: $\sim e^{-m_\pi L}$

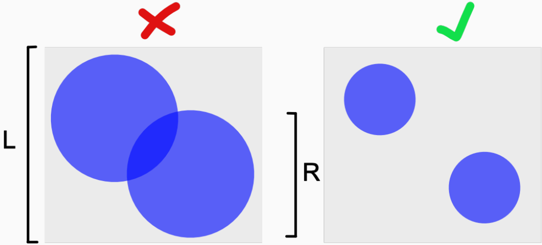

Steps in the calculation

- Lattice discretization of QCD ✓
- "Realistic operators" ✓
  - Quantum numbers ✓
  - Subduction ✓
  - Spatial smearing ✓
- Computing spectrum in finite box ✓
- Relating the spectrum to amplitudes ✓
- Parametrising amplitudes
- Fitting and finding poles

Amplitude constraints

s-channel unitarity: K matrix formalism

$$\boldsymbol{t} = \boldsymbol{K}(1 - i\boldsymbol{\rho}\boldsymbol{K})^{-1} \ .$$

Rotational symmetry: partial-wave expansion

$$t^l_{ab}(s) = \frac{1}{2}\int_{-1}^{1} d(\cos\theta) P_l(\cos\theta) t_{ab}(s,t) \ .$$

Threshold behaviour:

$$(\boldsymbol{t}^{-1})_{alS,bl'S'}(s) = (2k^{(a)}_{\text{cm}})^{-l}(\boldsymbol{K}^{-1})_{alS,bl'S'}(2k^{(b)}_{\text{cm}})^{-l'} - i\rho_a\delta_{ll'}\delta_{SS'}$$

Analyticity: Chew-Mandelstam phase space

$$\to t^{-1} = (2k_{\text{cm}})^{-l}K^{-1}(2k_{\text{cm}})^{-l'} + I(s)$$

$$I(s) = I(s_{\text{thr}}) + \frac{\rho}{\pi}\log\left[\frac{\xi + \rho(s)}{\xi(s) - \rho(s)}\right] - \frac{\xi(s)}{\pi}\frac{m_1 - m_2}{m_1 + m_2}\log\frac{m_2}{m_1}$$

with $\xi(s) = 1 - \frac{(m_1+m_2)^2}{s}$; subtracted at threshold

Fitting and pole-finding

Procedure:

- Parameterise the amplitude
- Determine the finite-volume spectrum from the determinant condition
- Compare the spectrum to the lattice result
- Change parameters and iterate to minimize the χ^2
  (using favourite numerical minimisation procedure)

Finally: analytically continue the result to the entire complex plane;
determine pole singularities in constrained amplitudes;
The location of the pole in the complex plane determines its physical significance, for example:

- Poles below threshold at real $s \leftrightarrow$ bound states
- Poles on the second sheet above threshold: $\sim$ resonances
- ...

Steps in the calculation

- Lattice discretization of QCD ✓
- "Realistic operators" ✓
  - Quantum numbers ✓
  - Subduction ✓
  - Spatial smearing ✓
- Computing spectrum in finite box ✓
- Relating the spectrum to amplitudes ✓
- Parametrising amplitudes ✓
- Fitting and finding poles ✓

$J^P = 0^+$: D_0^* and D_{s0}^*

- $m_{D_0^*} \gtrapprox m_{D_{s0}^*}$??
- What about the large width?

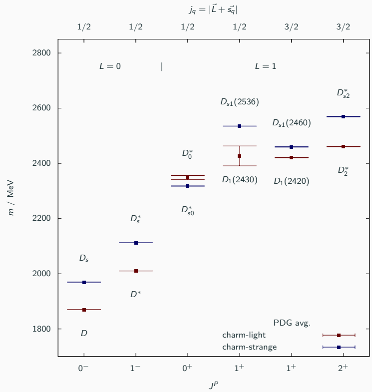

[Masses from PDG]

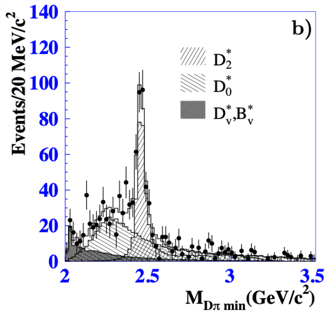

BELLE Collaboration [arXiv:hep-ex/0307021]

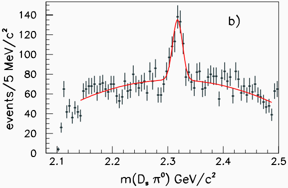

BABAR [arXiv:hep-ex/0304021]

- Energies extracted from fit of sum of exponentials to principal correlators
- Irreps labelled $[\vec{d}]\Lambda^{(P)}$ (overall momentum $\vec{P} = 2\pi\vec{d}/L$)
- At $\vec{P} = \vec{0}$:
  - $A_1^+ \leftrightarrow S$-wave
  - $T_1^- \leftrightarrow P$-wave
- Threshold suppression $\propto k^{2l}$: higher partial waves may be neglected
- Non-zero momentum $\rightarrow$ more mixing of partial waves

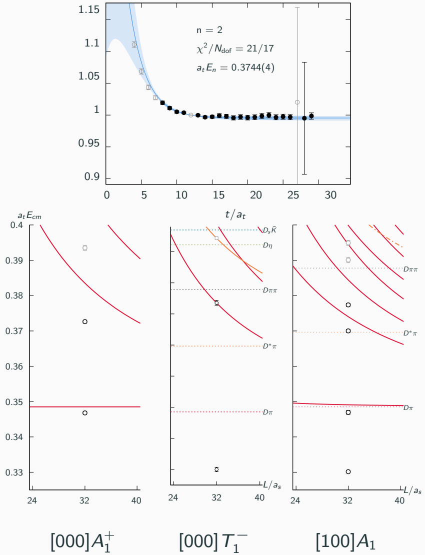

$D\pi$ at $m_\pi = 239$ MeV: Operator basis variations

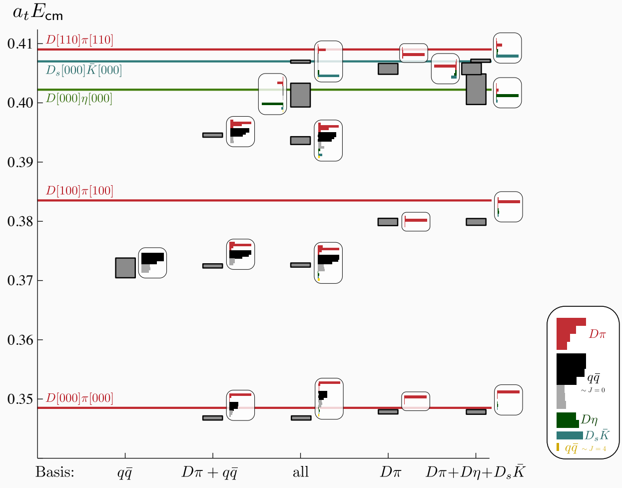

Spectrum in A_1^+

$\rightarrow$ A stable spectrum requires both $q\bar{q}$- and meson-meson-like operators!

$D\pi$ at $m_\pi = 239$ MeV: Parametrisations and poles

	$\ell = 0$ parameterisation	$\ell = 1$ parameterisation	N_{pars}	χ^2/N_{dof}
K-matrix with Chew-Mandelstam $I(s)$ in both partial waves				
ref.	$K = \frac{g^2}{m^2-s} + \gamma^{(0)}$	$K = \frac{g_1^2}{m_1^2-s}$	5	0.90
(a)	$K = \frac{g^2}{m^2-s}$	$K = \frac{g_1^2}{m_1^2-s}$	4	0.90
(b)	$K = \frac{g^2}{m^2-s} + \gamma^{(1)}\hat{s}$	$K = \frac{g_1^2}{m_1^2-s}$	5	0.90
(c)	$K = \frac{(g+g^{(1)}s)^2}{m^2-s}$	$K = \frac{g_1^2}{m_1^2-s}$	5	0.90
(d)	$K^{-1} = c^{(0)} + c^{(1)}\hat{s}$	$K = \frac{g_1^2}{m_1^2-s}$	4	0.90
(e)	$K^{-1} = \frac{c^{(0)}+c^{(1)}\hat{s}}{c^{(2)}\hat{s}}$	$K = \frac{g_1^2}{m_1^2-s}$	5	0.90
(f)	$K = \frac{g^2}{m^2-s} + \gamma^{(0)} + \gamma^{(1)}\hat{s}$	$K = \frac{g_1^2}{m_1^2-s}$	6	*0.94**
K-matrix with $I(s) = -i\rho(s)$ in both partial waves				
(g)	$K = \frac{g^2}{m^2-s} + \gamma^{(0)}$	$K = \frac{g_1^2}{m_1^2-s}$	5	0.90
(h)	$K = \frac{g^2}{m^2-s}$	$K = \frac{g_1^2}{m_1^2-s}$	4	0.91
(i)	$K = \frac{(g+g^{(1)}s)^2}{m^2-s}$	$K = \frac{g_1^2}{m_1^2-s}$	5	0.90
(j)	$K^{-1} = c^{(0)} + c^{(1)}\hat{s}$	$K = \frac{g_1^2}{m_1^2-s}$	4	0.91
(k)	$K^{-1} = \frac{c^{(0)}+c^{(1)}\hat{s}}{c^{(2)}\hat{s}}$	$K = \frac{g_1^2}{m_1^2-s}$	5	0.90
K-matrix with Chew-Mandelstam $I(s)$ in S-wave, Effective range in P-wave				
(l)	$K = \frac{g^2}{m^2-s} + \gamma^{(0)}$	$k\cot\delta_1 = 1/a_1 + \frac{1}{2}r_1^2k^2$	5	0.93
Effective range in S wave, K-matrix with Chew-Mandelstam $I(s)$ in P-wave				
(m)	$k\cot\delta_0 = 1/a_0 + \frac{1}{2}r_0^2k^2$	$K = \frac{g_1^2}{m_1^2-s}$	4	0.93
(n)	$k\cot\delta_0 = 1/a_0 + \frac{1}{2}r_0^2k^2 + P_{2,0}k^4$	$K = \frac{g_1^2}{m_1^2-s}$	5	*0.88*†
Effective range in both partial waves				
(o)	$k\cot\delta_0 = 1/a_0 + \frac{1}{2}r_0^2k^2$	$k\cot\delta_1 = 1/a_1 + \frac{1}{2}r_1^2k^2$	4	0.93
(p)	$k\cot\delta_0 = 1/a_0 + \frac{1}{2}r_0^2k^2 + P_{2,0}k^4$	$k\cot\delta_1 = 1/a_1 + \frac{1}{2}r_1^2k^2$	5	*0.91*†
Breit-Wigner in S-wave, K-matrix with Chew-Mandelstam $I(s)$ in P-wave				
(q)	$t = \frac{1}{\rho}\frac{m_R\Gamma_0}{m_R^2-s-im_R\Gamma_0}$	$K = \frac{g_1^2}{m_1^2-s}$	4	0.91
First-order unitarised χ_{PT}				
(s)	$t^{-1} = \left(-\frac{1}{16\pi}\mathcal{V}_{J=0}\right)^{-1} + 16\pi G_{\text{DR}}$	$K = \frac{g_1^2}{m_1^2-s}$	4	0.86

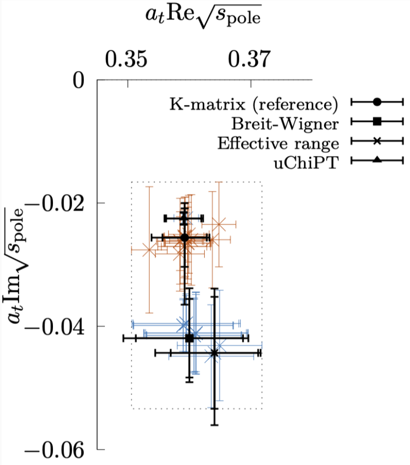

[L. Gayer, N. Lang et al (HadSpec), arXiv:2102.04973]

$D\pi$ at $m_\pi = 239$ MeV and $m_\pi = 391$ MeV

- $t \sim \frac{c^2}{s_{\text{pole}} - s}$
  $\sqrt{s} = m \pm \frac{i}{2}\Gamma$
- @$m_\pi = 391$ MeV:
  shallow bound-state
  $\approx 2 \pm 1$ MeV below threshold
- @$m_\pi = 239$ MeV: resonance
  $\approx 77 \pm 64$ MeV above threshold;
  below PDG value
  $\Gamma = 425 \pm 224$ MeV
- Strong coupling to $D\pi$ channel in both studies

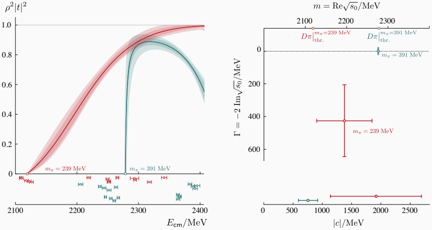

$$\sqrt{s_0}/\text{MeV} = (2196 \pm 64) - \frac{i}{2}(425 \pm 224)$$
$$c/\text{MeV} = (1916 \pm 776)\exp i\pi(-0.59 \pm 0.41)$$

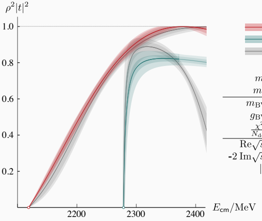

m_π/MeV	239	391
m_D/MeV	1880	1887
m_{BW}/MeV	2380(36)	2206(32)
g_{BW}	5.39(56)	7.62(75)
$\frac{\chi^2}{N_{\text{dof}}}$	$\frac{14.6}{20-4}$	$\frac{36.0}{29-5}$
$\text{Re}\sqrt{s_0}$/MeV	2189(72)	2275(1)
-2 $\text{Im}\sqrt{s_0}$/MeV	510(97)	-
$|c|$/MeV	2391(411)	826(133)

[L. Gayer, N. Lang et al (HadSpec), arXiv:2102.04973]
[G. Moir et al (HadSpec), JHEP 10 (2016) 011]

$I = 0$ DK at $m_\pi = 239$ MeV and $m_\pi = 391$ MeV

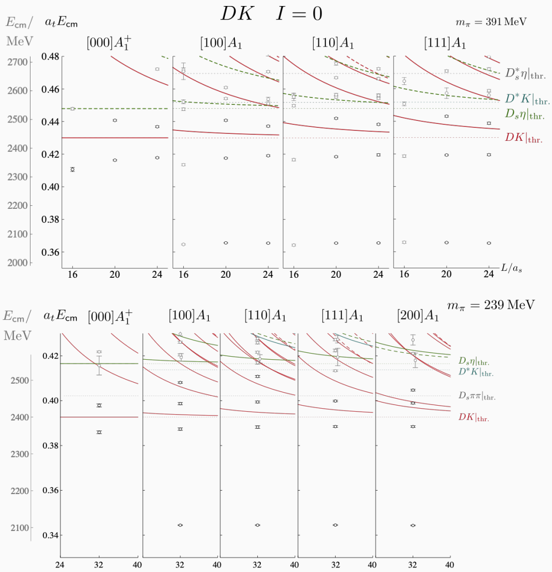

[G. Cheung et al (HadSpec), JHEP 02 (2021) 100 arXiv: 2008.06432]

$I = 0$ DK at $m_\pi = 239$ MeV and $m_\pi = 391$ MeV

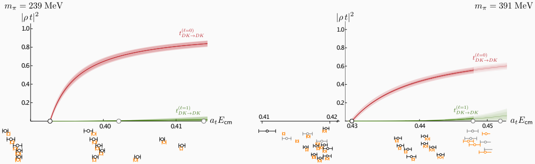

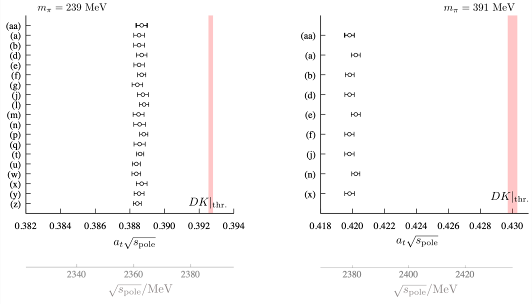

Bound states at both masses:

$m_\pi = 239$ MeV: $\sqrt{s} = 2362(3)$ MeV; $|c| = 1420(50)$ MeV

$m_\pi = 391$ MeV: $\sqrt{s} = 2380(3)$ MeV; $|c| = 1730(110)$ MeV

[G. Cheung et al (HadSpec), JHEP 02 (2021) 100 arXiv: 2008.06432]

Quark mass dependence

- *Natural* mass ordering
- Uχ_{PT}: many predictions of two-pole structure
- mass evolution of poles: SU(3)$_F$ $\rightarrow$ physical meson masses
- Poles in $\overline{\mathbf{3}}$ roughly consistent with lattice
- Higher sextet pole? Needs coupled-channel analysis

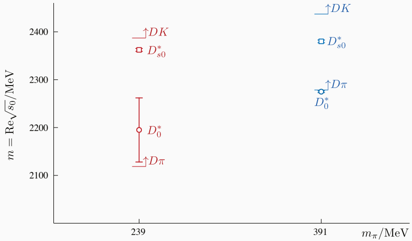

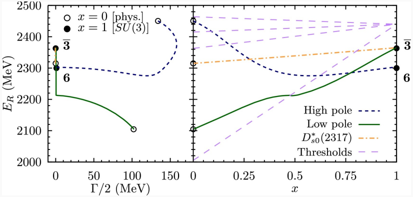

[Albaladejo et al., Physics Letters B, 767:465–469]

Heavy-light mesons with spin: $D^*\pi \to D^*\pi$ (Spectra)

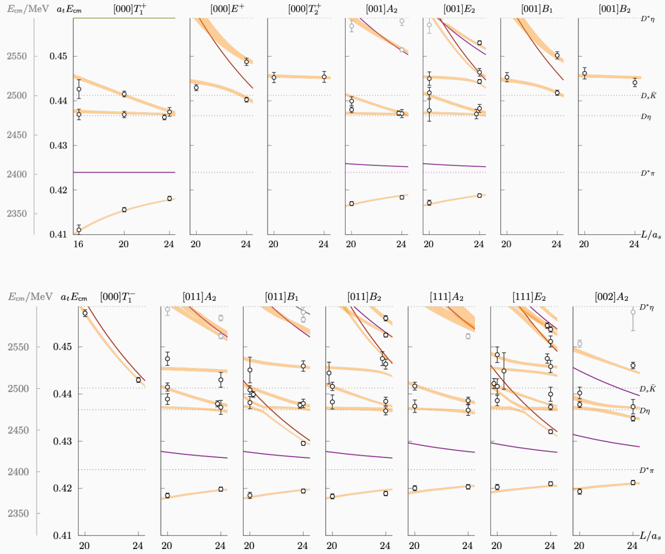

[N. Lang and D. Wilson (HadSpec) arXiv: 2205.05026]

$D^*\pi \to D^*\pi$ (Amplitudes)

$m_\pi = 391$ MeV

$$t_{J^P=1^+} = \begin{pmatrix} D^*\pi\{^3S_1 \to {}^3S_1\} & D^*\pi\{^3S_1 \to {}^3D_1\} \\ & D^*\pi\{^3D_1 \to {}^3D_1\} \end{pmatrix}$$

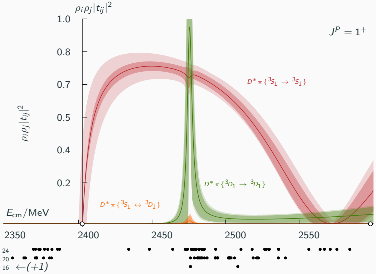

$$t_{J^P=2^+} = \begin{pmatrix} D\pi\{^1D_2 \to {}^1D_2\} & D\pi\{^1D_2\} \to D^*\pi\{^3D_2\} \\ & D^*\pi\{^3D_2 \to {}^3D_2\} \end{pmatrix}$$

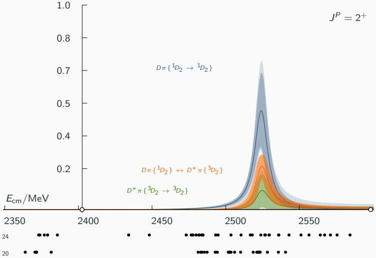

[N. Lang and D. Wilson (HadSpec) arXiv: 2205.05026]

$D^*\pi \to D^*\pi$ (Poles)

$m_\pi = 384$ MeV:

$\sqrt{s_{D_1}} = 2397(2)$ MeV — $\sqrt{s_{D_1}} = (2475(3) - \frac{i}{2}5(3))$ MeV — $\sqrt{s_{D_2}} = (2524(2) - \frac{i}{2}10(4))$ MeV;

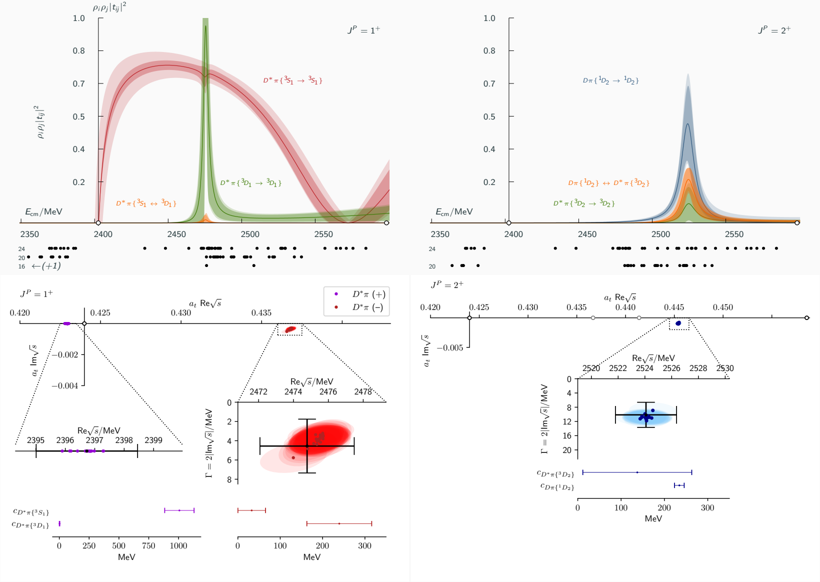

Conclusions

Lattice QCD provides *first principles* approach to hadron spectroscopy

- Well-established method in $2 \to 2$ scattering
- D-mesons: nice playground
  (experimental results available, interesting phenomenology, EFT descriptions...)
- Formalism applicable to wide range of processes (coupled-channels, charmonium, baryons...)
- There are challenges:
  - Lighter masses: computationally expensive + more open hadron-hadron channels
  - (3+)-body thresholds: formalism under development

Thank you! Questions?

Correlators on the lattice

- Compute matrix of (euclidean) correlators:

$$C_{ij}(t) = \langle 0|\mathcal{O}_i(t)\mathcal{O}_j^\dagger(0)|0\rangle \,,$$

- $\mathcal{O}_i(t)$ have quantum numbers of $I = 1/2\ D\pi$
- Find "optimal" interpolators by solving *Generalised Eigenvalue* (GEV) problem

$$C_{ij}(t)v_j^{(\mathfrak{n})} = \lambda_{\mathfrak{n}}(t, t_0)C_{ij}(t_0)v_j^{(\mathfrak{n})},$$

- Fit Principal correlators (eigenvalues):

$$\lambda_{\mathfrak{n}}(t, t_0) = (1 - A_{\mathfrak{n}})e^{-E_{\mathfrak{n}}(t-t_0)} + A_{\mathfrak{n}}e^{-E'_{\mathfrak{n}}(t-t_0)}.$$

Spatial smearing: Distillation

- Jacobi smearing: $J(t;\sigma,n_\sigma)=\left(1+\frac{\sigma\nabla^2(t)}{n_\sigma}\right)^{n_\sigma}$

  Laplace operator: $\nabla^2_{xy}(t)=-6\delta_{xy}+\sum_{j=1}^{3}\left(U_j(x,t)\delta_{x+\hat{j},y}+U_j^\dagger(x-\hat{j},t)\delta_{x-\hat{j},y}\right)$

$$\lim_{n_\sigma\to\infty} J(t;\sigma,n_\sigma)=Q(t)\exp\left[\sigma\Lambda(t)\right]Q^\dagger(t)$$

- Distillation operator:

$$\left[\Box(t)\right]_{xy}=\left[V(t)V^\dagger(t)\right]_{xy}=\sum_{k=1}^{N} v_x^{(k)}(t)v_y^{(k)\dagger}(t)$$

  $V(t)$: first N column vectors of $Q(t)$; $\sigma=0$

- Meson operator in distillation space:

$$C_M(t',t)=\langle\bar{q}'(t')\Box(t)\Gamma^B(t')\Box(t)q(t')\ \ \bar{q}(t)\Box(t)\Gamma^A(t)\Box(t)q'(t)\rangle$$

$$\to C_M^{\text{conn.}}(t',t)=\mathrm{Tr}\left[\phi^B(t')\tau(t',t)\phi^A(t)\tau(t,t')\right].$$

- Distillation space objects:

$$\phi^X_{\alpha\beta}(t)=V^\dagger(t)\Gamma^X_{\alpha\beta}(t)V(t)$$

$$\tau_{\alpha\beta}(t',t)=V^\dagger(t')M^{-1}_{\alpha\beta}(t',t)V(t)$$

Amplitude constraints: Unitarity

Define S matrix:

$$\boldsymbol{S} = \boldsymbol{1} + 2i\boldsymbol{\rho t}$$

Unitarity of S matrix:

$$\boldsymbol{1} = \boldsymbol{S}\boldsymbol{S}^\dagger$$
$$\boldsymbol{t} - \boldsymbol{t}^\dagger = 2i\boldsymbol{t\rho t}^\dagger$$

For a single kinematically open channel:

$$t_a(s) = e^{i\delta_a} \sin\delta_a / \rho_a$$

Is there a parametrisation that automatically respects unitarity?

$$\left(\boldsymbol{t}^\dagger\right)^{-1} - \boldsymbol{t}^{-1} = 2i\boldsymbol{\rho}$$
$$\boldsymbol{t}^{-1} = \boldsymbol{K}^{-1} - i\boldsymbol{\rho}\ ,$$
$$\boldsymbol{t} = \boldsymbol{K}(1 - i\boldsymbol{\rho K})^{-1}\ .$$

K is real and has no branch cut singularities
For a single kinematically open channel:

$$K_a = \tan\delta_a$$

Amplitude constraints: rotational symmetry

Spherically symmetric potential: $V(x) = V(|x|)$
$\psi(r) \sim R(|x|) Y_{lm}(\hat{x})$

$$\to t_{ab}(s,t) = \sum_l (2l+1) P_l\big(\cos\theta(s,t)\big)\, t^l_{ab}(s)$$

with

$$t^l_{ab}(s) = \frac{1}{2}\int_{-1}^{1} d(\cos\theta) P_l(\cos\theta) t_{ab}(s,t)\ .$$

In case of non-mixing channels:

$$t^l_{ab}(s) = e^{i\delta^l_a} \sin\delta / \rho_a \delta_{a,b}$$

For the K matrix:

$$(\boldsymbol{t}^{-1})_{alS,bl'S'}(s) = (\boldsymbol{K}^{-1})_{alS,bl'S'} - i\rho_a \delta_{ll'}\delta_{SS'}$$

($\boldsymbol{t}$ and $\boldsymbol{K}$ are block-diagonal in $\vec{J} = \vec{L} + \vec{S}$)

Amplitude constraints: Threshold behaviour and effective range

As $k_{\mathrm{cm}} \to 0$: $\delta_l \to -a_l k_{\mathrm{cm}}^{2l+1}$

$$K_l \to -a_l k_{\mathrm{cm}}^{2l+1}$$

We can build this into the K matrix definition:

$$(\boldsymbol{t}^{-1})_{alS,bl'S'}(s) = (2k_{\mathrm{cm}}^{(a)})^{-l}(\boldsymbol{K}^{-1})_{alS,bl'S'}(2k_{\mathrm{cm}}^{(b)})^{-l'} - i\rho_a \delta_{ll'}\delta_{SS'}$$

K even, analytic function of k_{cm} near threshold $\to$ for single channel:

$$(k_{\mathrm{cm}})^{2l+1} \cot \delta_l = \frac{1}{a_l} + \frac{1}{2} r_{0,l}(k_{\mathrm{cm}})^2 + \mathcal{O}((k_{\mathrm{cm}})^4)$$

- Effective range expansion
- a_l is called scattering length
- $r_{0,l} \sim$ range of potential (for $l = 0$)

The Chew-Mandelstam phase space

Can we make use of analyticity?

Cauchy's theorem:

$$f(s) = \frac{1}{2\pi i}\int_{(m_1+m_2)^2}^{\infty} ds' \frac{f(s'+i\epsilon) - f(s'-i\epsilon)}{s'-s}$$
$$= -\frac{1}{\pi}\int_{(m_1+m_2)^2}^{\infty} ds' \frac{\rho(s)}{s'-s} \equiv I(s)$$

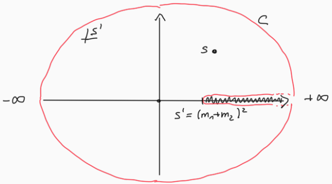

Regularize through subtraction:

$$t^{-1} = I(s_0) + [I(s) - I(s_0)]$$
$$= I(s_0) - \frac{(s-s_0)}{\pi}\int \frac{\rho(s)ds'}{(s'-s_0)(s'-s)}$$
$$\rightarrow t^{-1} = (2k_{\mathrm{cm}})^{-l} K^{-1} (2k_{\mathrm{cm}})^{-l'} + I(s)$$

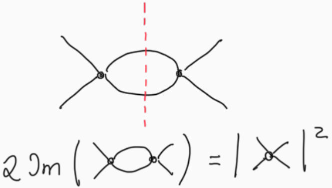

Result: Chew-Mandelstam phase space

$$I(s) = I(s_{\mathrm{thr}}) + \frac{\rho}{\pi}\log\left[\frac{\xi + \rho(s)}{\xi(s) - \rho(s)}\right] - \frac{\xi(s)}{\pi}\frac{m_1 - m_2}{m_1 + m_2}\log\frac{m_2}{m_1}$$

with $\xi(s) = 1 - \frac{(m_1+m_2)^2}{s}$; subtracted at threshold

$D\pi$ at $m_\pi = 239$ MeV: Correlators

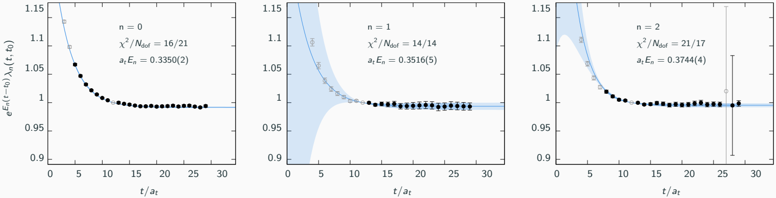

Principal correlators in $[100]A_1$; Leading exponential divided out

- Typically fit of sum of two exponentials (excited state contamination)
- Chosen from a range of different fits
- Uncertainties across fits accounted for in spectrum

Ensembles

a_s	0.11 fm
a_t^{-1}	6.079 GeV
$(L/a_s)^3 \times (T/a_t)$	$32^3 \times 256$
m_π	239 MeV
N_f	$2+1$
N_{cfg}	484

a_s	0.12 fm
a_t^{-1}	5.667 GeV
$(L/a_s)^3 \times (T/a_t)$	$\{16^3, 20^3, 24^3\} \times 256$
m_π	391 MeV
N_f	$2+1$
N_{cfg}	$\{479, 603, 552\}$

$D\pi$ 239 MeV Operator Table (S-wave)

$A_1^+[000]$	$A_1[100]$	$A_1[110]$	$A_1[111]$	$A_1[200]$
$D_{[000]}\ \pi_{[000]}$	$D_{[000]}\ \pi_{[100]}$	$D_{[000]}\ \pi_{[110]}$	$D_{[000]}\ \pi_{[111]}$	$D_{[100]}\ \pi_{[100]}$
$D_{[100]}\ \pi_{[100]}$	$D_{[100]}\ \pi_{[000]}$	$D_{[100]}\ \pi_{[100]}$	$D_{[100]}\ \pi_{[110]}$	$D_{[110]}\ \pi_{[110]}$
$D_{[110]}\ \pi_{[110]}$	$D_{[100]}\ \pi_{[110]}$	$D_{[110]}\ \pi_{[000]}$	$D_{[110]}\ \pi_{[100]}$	$D_{[200]}\ \pi_{[000]}$
$D_{[111]}\ \pi_{[111]}$	$D_{[100]}\ \pi_{[200]}$	$D_{[110]}\ \pi_{[110]}$	$D_{[111]}\ \pi_{[000]}$	$D_{[210]}\ \pi_{[100]}$
$D_{[000]}\ \eta_{[000]}$	$D_{[110]}\ \pi_{[100]}$	$D_{[111]}\ \pi_{[100]}$	$D_{[211]}\ \pi_{[100]}$	$D_{[200]}\ \eta_{[000]}$
$D_{[100]}\ \eta_{[100]}$	$D_{[110]}\ \pi_{[111]}$	$D_{[210]}\ \pi_{[100]}$	$D^*_{[110]}\ \pi_{[100]}$	
$D_{s[000]}\ \bar{K}_{[000]}$	$D_{[111]}\ \pi_{[110]}$	$D^*_{[100]}\ \pi_{[100]}$	$D_{[111]}\ \eta_{[000]}$	
	$D_{[200]}\ \pi_{[100]}$	$D^*_{[111]}\ \pi_{[100]}$	$D_{s[111]}\ \bar{K}_{[000]}$	
	$D_{[210]}\ \pi_{[110]}$	$D_{[110]}\ \eta_{[000]}$		
	$D_{[000]}\ \eta_{[100]}$	$D_{s[110]}\ \bar{K}_{[000]}$		
	$D_{[100]}\ \eta_{[000]}$			
	$D_{s[000]}\ \bar{K}_{[100]}$			
	$D_{s[100]}\ \bar{K}_{[000]}$			
$8 \times \bar{\psi}\mathbf{\Gamma}\psi$	$18 \times \bar{\psi}\mathbf{\Gamma}\psi$	$18 \times \bar{\psi}\mathbf{\Gamma}\psi$	$9 \times \bar{\psi}\mathbf{\Gamma}\psi$	$16 \times \bar{\psi}\mathbf{\Gamma}\psi$

Operators used in the S-wave fits. Subscripts indicate momentum types. $\mathbf{\Gamma}$ represents some monomial of γ matrices and derivatives.

$D\pi$ 239 MeV Operator Table (P-wave)

T_1^-[000]	E_2[100]	B_1[110]	B_2[110]
$D_{[100]}\ \pi_{[100]}$	$D_{[100]}\ \pi_{[110]}$	$D_{[100]}\ \pi_{[100]}$	$D_{[100]}\ \pi_{[111]}$
$D_{[110]}\ \pi_{[110]}$	$D_{[110]}\ \pi_{[100]}$	$D_{[110]}\ \pi_{[110]}$	$D_{[110]}\ \pi_{[110]}$
$D^*_{[100]}\ \pi_{[100]}$	$D^*_{[000]}\ \pi_{[100]}$	$D_{[210]}\ \pi_{[100]}$	$D_{[111]}\ \pi_{[100]}$
	$D^*_{[100]}\ \pi_{[000]}$	$D^*_{[100]}\ \pi_{[100]}$	$D^*_{[000]}\ \pi_{[110]}$
		$D^*_{[110]}\ \pi_{[000]}$	$D^*_{[100]}\ \pi_{[100]}\ \{2\}$
			$D^*_{[110]}\ \pi_{[000]}$
			$D^*_{[111]}\ \pi_{[100]}$
$6 \times \bar{\psi}\mathbf{\Gamma}\psi$	$18 \times \bar{\psi}\mathbf{\Gamma}\psi$	$18 \times \bar{\psi}\mathbf{\Gamma}\psi$	$20 \times \bar{\psi}\mathbf{\Gamma}\psi$

Operators used in the P-wave fits. Subscripts indicate momentum types. $\mathbf{\Gamma}$ represents some monomial of γ matrices and derivatives. The number in curly parentheses indicates the number of operators of this momentum combination.

$D^*\pi$ 391 MeV Operator Table (part 1)

$[000]T_1^+$	$[000]E^+$	$[000]T_2^+$	$[001]A_2$	$[001]E_2$	$[001]B_1$	$[001]B_2$
$D_{[000]}\rho_{[000]}$ (1)	$D_{[100]}\pi_{[100]}$ (1)	$D_{[110]}\pi_{[110]}$ (1)	$D_{[100]}\rho_{[000]}$ (1)	$D_{[100]}\pi_{[110]}$ (1)	$D_{[100]}\pi_{[110]}$ (1)	$D_{[111]}\pi_{[110]}$ (1)
$D_{[100]}\rho_{[100]}$ (2)	$D_{[110]}\pi_{[110]}$ (1)	$D^*{}_{[100]}\pi_{[100]}$ (1)	$D_{[000]}f_{0\,[100]}$ (1)	$D_{[110]}\pi_{[100]}$ (1)	$D_{[110]}\pi_{[100]}$ (1)	$D_{[110]}f_{0\,[100]}$ (1)
$D_{[100]}f_{0\,[100]}$ (1)	$D_{[200]}\pi_{[200]}$ (1)	$D^*{}_{[000]}\rho_{[000]}$ (1)	$D_{[100]}f_{0\,[000]}$ (1)	$D_{[111]}\pi_{[110]}$ (1)	$D_{[100]}\eta_{[110]}$ (1)	$D^*{}_{[100]}\pi_{[110]}$ (2)
$D^*{}_{[000]}\pi_{[000]}$ (1)	$D_{[100]}\eta_{[100]}$ (1)	$\bar{q}\boldsymbol{\Gamma}q$ (29)	$D^*{}_{[000]}\pi_{[100]}$ (1)	$D_{[110]}\eta_{[100]}$ (1)	$D_{[110]}\eta_{[100]}$ (1)	$D^*{}_{[110]}\pi_{[100]}$ (2)
$D^*{}_{[100]}\pi_{[100]}$ (2)	$D_{[110]}\eta_{[110]}$ (1)		$D^*{}_{[100]}\pi_{[000]}$ (1)	$D_{[000]}\rho_{[100]}$ (1)	$D_{s\,[100]}\bar{K}_{[110]}$ (1)	$\bar{q}\boldsymbol{\Gamma}q$ (20)
$D^*{}_{[110]}\pi_{[110]}$ (3)	$D_{s\,[100]}\bar{K}_{[100]}$ (1)		$D^*{}_{[110]}\pi_{[100]}$ (2)	$D_{[100]}\rho_{[000]}$ (1)	$D_{s\,[110]}\bar{K}_{[100]}$ (1)	
$D^*{}_{[000]}\eta_{[000]}$ (1)	$D_{s\,[110]}\bar{K}_{[110]}$ (1)		$D^*{}_{[100]}\eta_{[000]}$ (1)	$D_{s\,[110]}\bar{K}_{[100]}$ (1)	$\bar{q}\boldsymbol{\Gamma}q$ (12)	
$D^*{}_{[100]}\eta_{[100]}$ (2)	$\bar{q}\boldsymbol{\Gamma}q$ (4)		$D^*_{s\,[100]}\bar{K}_{[000]}$ (1)	$D^*{}_{[000]}\pi_{[100]}$ (1)		
$D^*{}_{[000]}\rho_{[000]}$ (1)			$D_{0\,[100]}\pi_{[000]}$ (1)	$D^*{}_{[100]}\pi_{[000]}$ (1)		
$D^*_{s\,[000]}\bar{K}_{[000]}$ (1)			$\bar{q}\boldsymbol{\Gamma}q$ (32)	$D^*{}_{[110]}\pi_{[100]}$ (3)		
$D^*_{s\,[100]}\bar{K}_{[100]}$ (2)				$D^*{}_{[000]}\eta_{[100]}$ (1)		
$D_{0\,[100]}\pi_{[100]}$ (1)				$D^*{}_{[100]}\eta_{[000]}$ (1)		
$\bar{q}\boldsymbol{\Gamma}q$ (44)				$D^*{}_{[100]}f_{0\,[000]}$ (1)		
				$D^*_{s\,[100]}\bar{K}_{[000]}$ (1)		
				$\bar{q}\boldsymbol{\Gamma}q$ (44)		

$I = 1/2$ $D^*\pi$-, $D^*\eta$- and $D_s^*\bar{K}$-like operators

$D^*\pi$ 391 MeV Operator Table (part 2)

$[000]T_1^-$	$[011]A_2$	$[011]B_1$	$[011]B_2$	$[111]A_2$	$[111]E_2$	$[002]A_2$
$D_{[100]}\pi_{[100]}$ (1)	$D_{[110]}\pi_{[110]}$ (1)	$D_{[100]}\pi_{[100]}$ (1)	$D_{[110]}\pi_{[110]}$ (1)	$D_{[111]}\rho_{[000]}$ (1)	$D_{[100]}\pi_{[110]}$ (1)	$D_{[100]}\rho_{[100]}$ (1)
$D_{[100]}\eta_{[100]}$ (1)	$D_{[110]}\rho_{[000]}$ (1)	$D_{[110]}\pi_{[110]}$ (1)	$D_{[111]}\pi_{[100]}$ (1)	$D_{[111]}f_{0\,[000]}$ (1)	$D_{[110]}\pi_{[100]}$ (1)	$D_{[100]}f_{0\,[100]}$ (1)
$D^*_{[100]}\pi_{[100]}$ (1)	$D_{[110]}f_{0\,[000]}$ (1)	$D_{[210]}\pi_{[100]}$ (1)	$D_{[110]}\rho_{[000]}$ (1)	$D^*_{[110]}\pi_{[100]}$ (2)	$D_{[211]}\pi_{[100]}$ (1)	$D_{[200]}f_{0\,[000]}$ (1)
$\bar{q}\mathbf{\Gamma}q$ (20)	$D^*_{[100]}\pi_{[100]}$ (2)	$D_{[100]}\eta_{[100]}$ (1)	$D_{[100]}f_{0\,[100]}$ (1)	$D^*_{[111]}\pi_{[000]}$ (1)	$D_{[100]}\eta_{[110]}$ (1)	$D^*_{[100]}\pi_{[100]}$ (1)
	$D^*_{[110]}\pi_{[000]}$ (1)	$D_{[110]}\rho_{[000]}$ (1)	$D^*_{[000]}\pi_{[110]}$ (1)	$D^*_{[111]}\eta_{[000]}$ (1)	$D_{[110]}\eta_{[100]}$ (1)	$D^*_{[200]}\pi_{[000]}$ (1)
	$D^*_{[111]}\pi_{[100]}$ (2)	$D_{s\,[100]}\bar{K}_{[100]}$ (1)	$D^*_{[100]}\pi_{[100]}$ (2)	$D^*_{s\,[111]}\bar{K}_{[000]}$ (1)	$D_{[111]}\rho_{[000]}$ (1)	$D^*_{[210]}\pi_{[100]}$ (2)
	$D^*_{[110]}\eta_{[000]}$ (1)	$D^*_{[000]}\pi_{[110]}$ (1)	$D^*_{[110]}\pi_{[000]}$ (1)	$D_{0\,[111]}\pi_{[000]}$ (1)	$D_{[110]}f_{0\,[100]}$ (1)	$D^*_{[100]}\eta_{[100]}$ (1)
	$D^*_{s\,[110]}\bar{K}_{[000]}$ (1)	$D^*_{[100]}\pi_{[100]}$ (1)	$D^*_{[111]}\pi_{[100]}$ (1)	$\bar{q}\mathbf{\Gamma}q$ (36)	$D_{s\,[100]}\bar{K}_{[110]}$ (1)	$D^*_{[200]}\eta_{[000]}$ (1)
	$D_{0\,[110]}\pi_{[000]}$ (1)	$D^*_{[110]}\pi_{[000]}$ (1)	$D^*_{[110]}\eta_{[000]}$ (1)		$D_{s\,[110]}\bar{K}_{[100]}$ (1)	$D^*_{s\,[200]}\bar{K}_{[000]}$ (1)
	$\bar{q}\mathbf{\Gamma}q$ (52)	$D^*_{[111]}\pi_{[100]}$ (2)	$D^*_{s\,[110]}\bar{K}_{[000]}$ (1)		$D^*_{[100]}\pi_{[110]}$ (3)	$\bar{q}\mathbf{\Gamma}q$ (32)
		$D^*_{[100]}\eta_{[100]}$ (1)	$\bar{q}\mathbf{\Gamma}q$ (52)		$D^*_{[110]}\pi_{[100]}$ (3)	
		$D^*_{[110]}\eta_{[000]}$ (1)			$D^*_{[111]}\pi_{[000]}$ (1)	
		$D^*_{[110]}f_{0\,[000]}$ (1)			$D^*_{[111]}\eta_{[000]}$ (1)	
		$D^*_{s\,[110]}\bar{K}_{[000]}$ (1)			$D^*_{s\,[111]}\bar{K}_{[000]}$ (1)	
		$\bar{q}\mathbf{\Gamma}q$ (44)			$\bar{q}\mathbf{\Gamma}q$ (60)	

$I = 1/2$ $D^*\pi$-, $D^*\eta$- and $D_s^*\bar{K}$-like operators

Subduction Table (1)

$\vec{P}$	Irrep Λ	J^P $(\vec{P}=\vec{0})$ $\lvert\lambda\rvert^{(\tilde{\eta})}$ $(\vec{P}\neq\vec{0})$	$D\pi$ $J^P_{[N]}$	$D^*\pi$ $J^P_{[N]}$
[000]	A_1^+	0^+, 4^+	0^+, ...	...
	T_1^-	1^-, 3^-	1^-, ...	...
	E^+	2^+, 4^+	2^+, ...	...
$[n00]$	A_1	$0^{(+)}$, 4	0^+, 1^-, 2^+, ...	...
	E_2	1, 3	1^-, 2^+, ...	1^+, ...
$[nn0]$	A_1	$0^{(+)}$, 2, 4	0^+, 1^-, $2^+_{[2]}$, ...	...
	$B_2,\ B_2$	1, 3	1^-, 2^+, ...	1^+, ...
$[nnn]$	A_1	$0^{(+)}$, 3	0^+, 1^-, 2^+, ...	...

Lowest $D\pi$ and $D^*\pi$ continuum J^P and helicity λ subductions by irrep

Subduction Table (2)

$\vec{d}$	G	Λ	J^P $(\vec{P}=\vec{0})$ $\lvert\lambda\rvert^{(\tilde{\eta})}$ $(\vec{P}\neq\vec{0})$	${}^1\ell_J$	${}^3\ell_J$
[000]	O_h	A_1^+	0^+, ...	${}^1S_0$	
		A_2^+	3^+, ...		${}^3D_3$
		E^+	2^+, ...	${}^1D_2$	${}^3D_2$
		T_1^+	1^+, 3^+, ...		$({}^3S_1, {}^3D_1)$, ${}^3D_3$
		T_2^+	2^+, ...	${}^1D_2$	${}^3D_2$, ${}^3D_3$
		A_1^-	0^-, ...		${}^3P_0$
		A_2^-	3^-, ...	...	...
		E^-	2^-, ...		${}^3P_2$
		T_1^-	1^-, 3^-, ...	${}^1P_1$	${}^3P_1$
		T_2^-	2^-, ...		${}^3P_2$
$[n00]$	C_{4v}	A_2	$0^{(-)}$, $1^{(+)}$, $2^{(-)}$, $3^{(+)}$		${}^3P_0$, $({}^3S_1, {}^3D_1)$, ${}^3P_2$, ${}^3D_3$
		B_1, B_2	2, 3	${}^1D_2$	${}^3D_2$, ${}^3P_2$, ${}^3D_2$
		E_2	1, 2, 3	${}^1P_1$, ${}^1D_2$	$({}^3S_1, {}^3D_1)$, ${}^3P_1$, ${}^3D_2$, ${}^3P_2$, ${}^3D_3$
$[nn0]$	C_{2v}	A_2	$0^{(-)}$, $1^{(+)}$, 2, 3	${}^1D_2$	${}^3P_0$, $({}^3S_1, {}^3D_1)$, ${}^3D_2$, ${}^3P_2$, ${}^3D_3$
		B_1, B_2	1, 2, 3	${}^1P_1$, ${}^1D_2$	$({}^3S_1, {}^3D_1)$, ${}^3P_1$, ${}^3D_2$, ${}^3P_2$, ${}^3D_3$
$[nnn]$	C_{3v}	A_2	$0^{(-)}$, $1^{(+)}$, 2^-, 3		${}^3P_0$, $({}^3S_1, {}^3D_1)$, ${}^3P_2$, ${}^3D_3$
		E_2	1, 2, 3	${}^1P_1$, ${}^1D_2$	$({}^3S_1, {}^3D_1)$, ${}^3D_2$, ${}^3P_2$, ${}^3D_3$

Lattice symmetry groups and partial-wave subductions for vector-pseudoscalar scattering

Masses and thresholds ($m_\pi = 239$ MeV)

	$a_t m$
π	0.03928(18)
K	0.08344(7)
η	0.09299(56)
D	0.30923(11)
D_s	0.32356(12)
D^*	0.33058(24)

	$a_t E_{\mathrm{threshold}}$
$D\pi$	0.34851(21)
$D\pi\pi$	0.38779(27)
$D\eta$	0.40222(57)
$D_s\bar{K}$	0.40700(14)
$D^*\pi\pi$	0.40914(35)

Left: Stable hadron masses. Right: kinematic thresholds.

Masses and thresholds ($m_\pi = 391$ MeV)

	$a_t m$
π	0.06906(13)
K	0.09698(9)
η	0.10364(19)
D	0.33303(31)
D_s	0.34441(29)
D^*	0.35494(46)
D_s^*	0.36587(35)

	$a_t E_{\mathrm{threshold}}$	$E_{\mathrm{threshold}}$/MeV
$D\pi$	0.40209(34)	2278.6 ± 1.9
$D^*\pi$	0.4240(5)	2402.8 ± 2.7
$D^*\eta$	0.4586(5)	2598.8 ± 2.8
$D_s^*\bar{K}$	0.4629(4)	2623.0 ± 2.0
$D\pi\pi$	0.4711(4)	2670.0 ± 2.3
$D^*\pi\pi$	0.4931(5)	2794.2 ± 3.0

Left: Stable hadron masses. Right: kinematic thresholds.

Operator basis variations

- Varying the basis affects the spectrum
- $I = 1/2$ allows both meson-meson and $q\bar{q}$-like operator constructions
- Interpolating the complete spectrum requires both types of operator
- Other meson-meson operators do not play a significant role below coupled-channel threshold

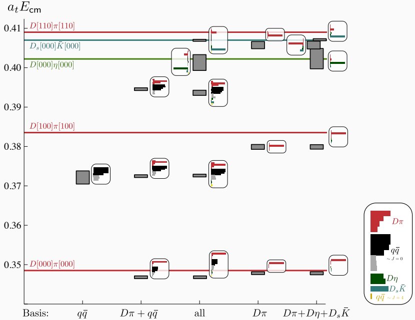

Spectrum in A_1^+

SU(3) point

Consider $SU(3)_F$ symmetric theory ($m_u = m_d = m_s$):

- meson-meson system transforms like $\bar{\mathbf{3}} \otimes \mathbf{8} = \bar{\mathbf{3}} \oplus \mathbf{6} \oplus \overline{\mathbf{15}}$ under flavour rotations
- For broken flavour symmetry these representations mix: $D^{(*)}\pi$ / $D^{(*)}\eta$ / $D_s^{(*)}\bar{K}$ receive contributions from all three

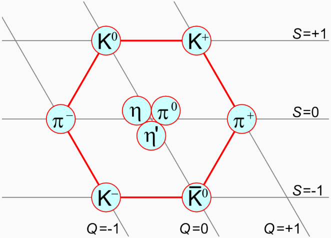

https://en.wikipedia.org/wiki/Quark_model - Public Domain

Heavy-quark symmetry

- $m_c = m_Q \to \infty$
  $\Rightarrow -igT^a\gamma^\mu \to -igT^a v^\mu + \mathcal{O}(1/m_Q)$
  (heavy-quark spin symmetry)
  $\Rightarrow U(N_h)_F$
  (heavy-flavour symmetry)
- Spins decoupled; define:
  $\vec{j_l} \equiv \vec{J} - \vec{S_Q} = \vec{L} + \vec{S_q}$
- For $L = 1$ we get: $j_l = 1/2$ and $j_l = 3/2$
- This gives:
  $\mathbf{2} \otimes \mathbf{2} = \mathbf{1} \oplus \mathbf{3}$ and $\mathbf{2} \otimes \mathbf{4} = \mathbf{3} \oplus \mathbf{5}$
- $\Rightarrow$ Two positive parity spin doublets:
  $(0^+, 1^+)$ and $(1^+, 2^+)$